

Nuclear shape / phase transitions in the $N = 40, 60, 90$ regions

Adam Prášek^a, Petr Alexa^a, Dennis Bonatsos^b, Dimitrios Petrellis^c,
Gabriela Thiamová^d, Petr Veselý^c

^aDepartment of Physics, VŠB, Technical University Osrtava

^bInstitute of Nuclear and Particle Physics, N.C.S.R. "Demokritos"^c

^cNuclear Physics Institute, Czech Academy of Sciences

^dUniversite Grenoble 1, CNRS, LPSC, Institute Polytechnique de Grenoble, IN2P3

This work is dedicated to the memory of Adam Prášek

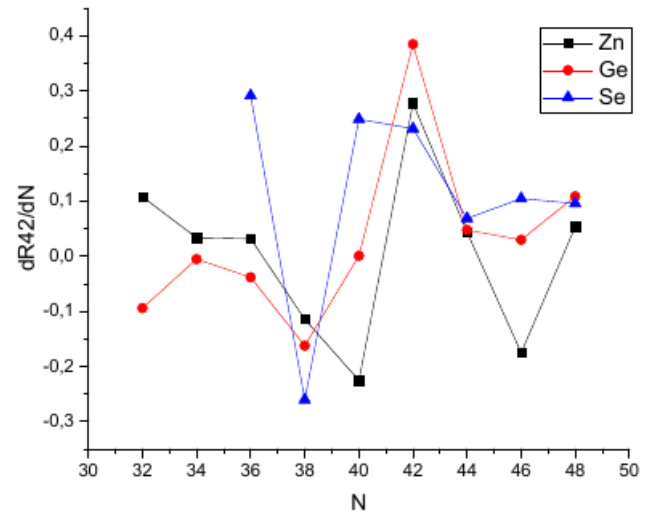
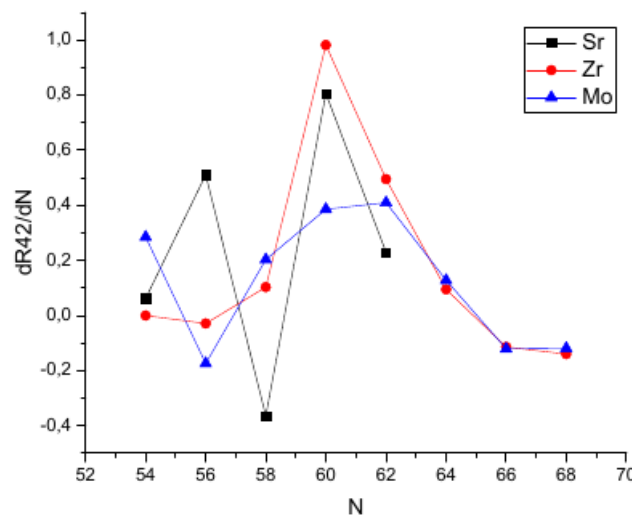
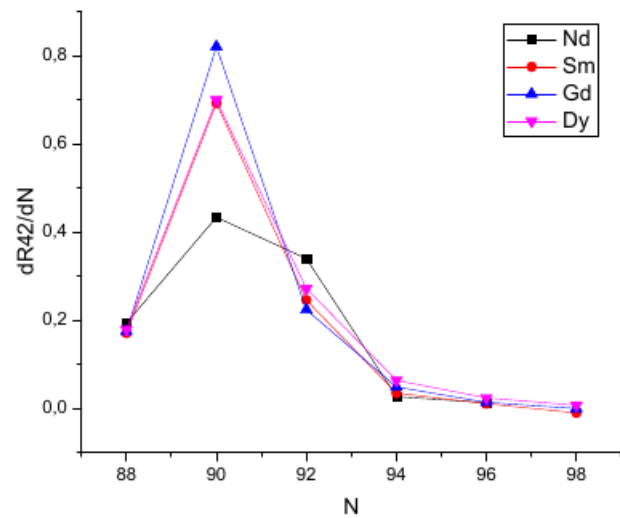
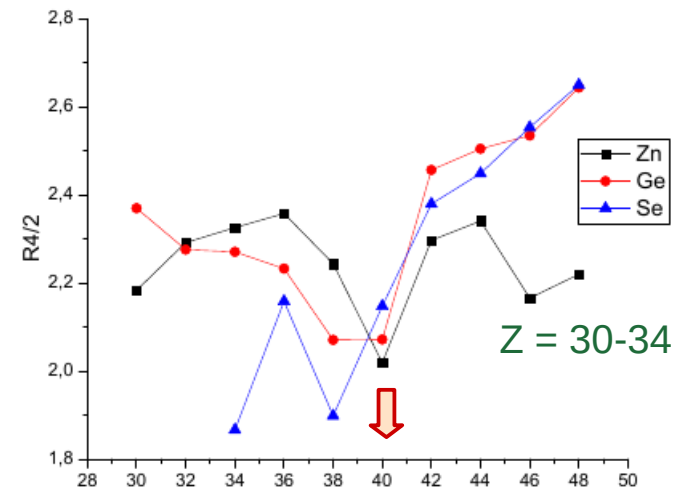
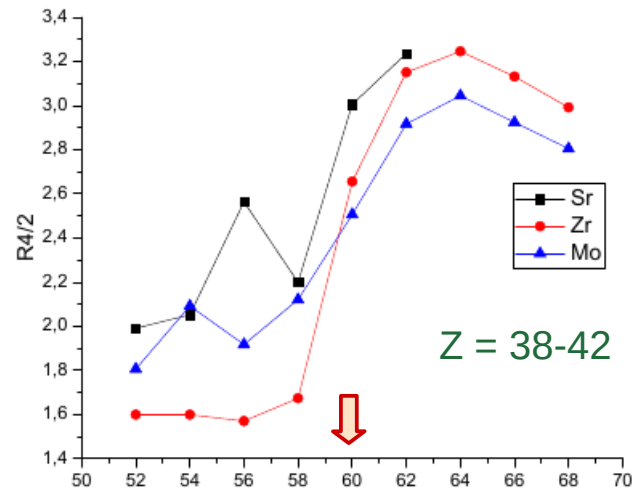
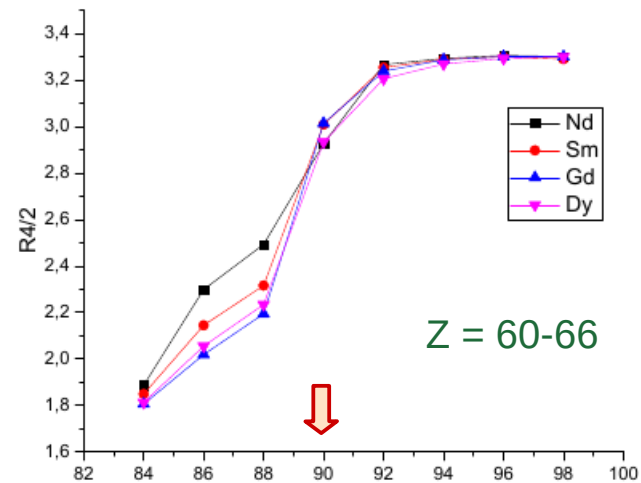
Outline

- Manifestations of structural change
- Shell model interpretation
- Microscopic self-consistent calculations
- Algebraic Collective Model calculations

Energy ratios $R_{4/2}$

$$R_{4/2} = \frac{E(4_1^+)}{E(2_1^+)}$$

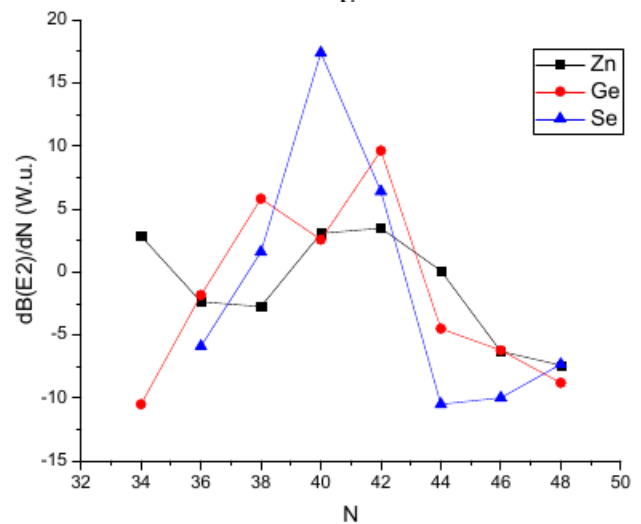
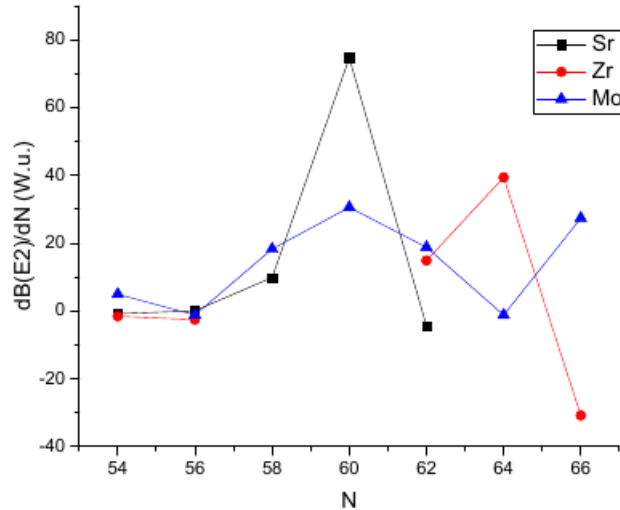
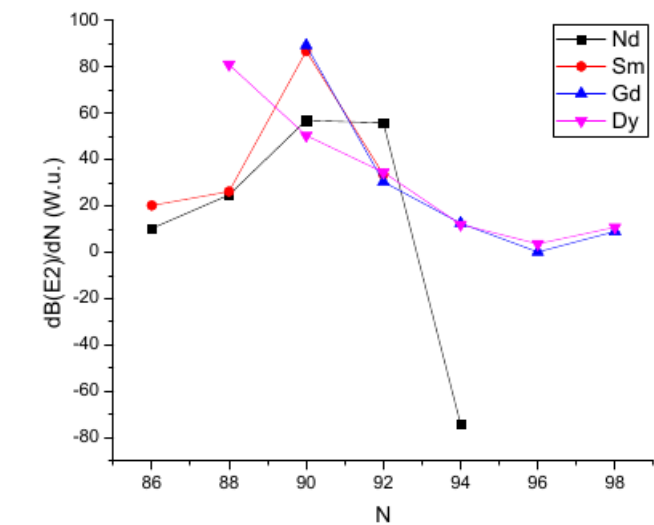
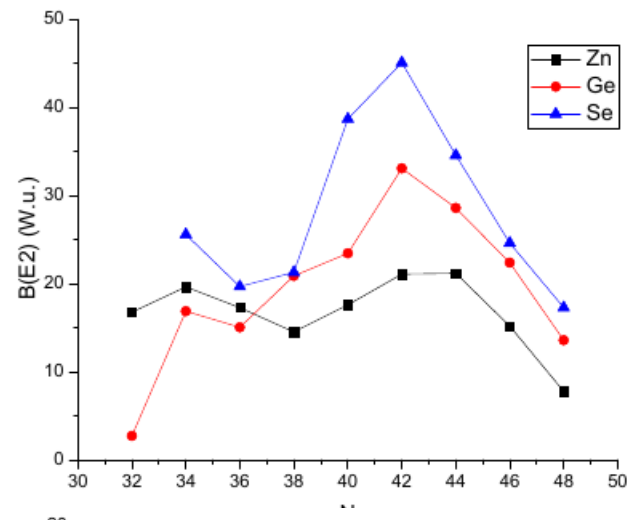
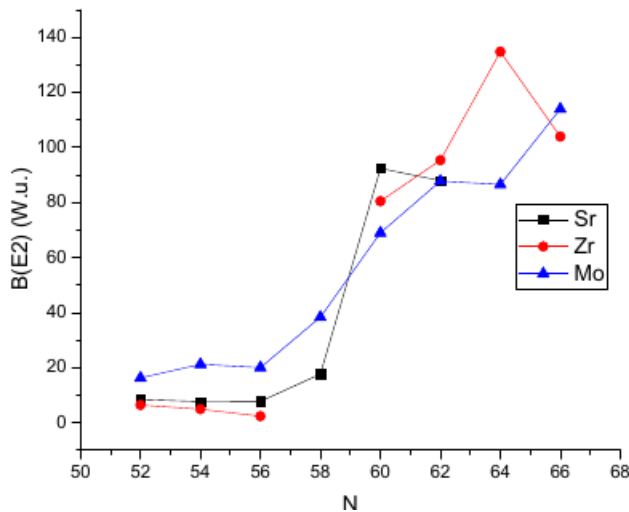
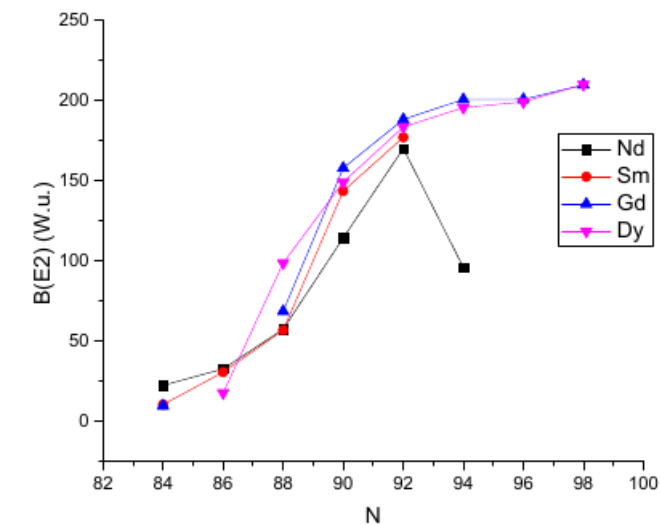
$$\frac{dR_{4/2}}{dN}(N) = R_{4/2}(N) - R_{4/2}(N-2)$$



B(E2) transition rates

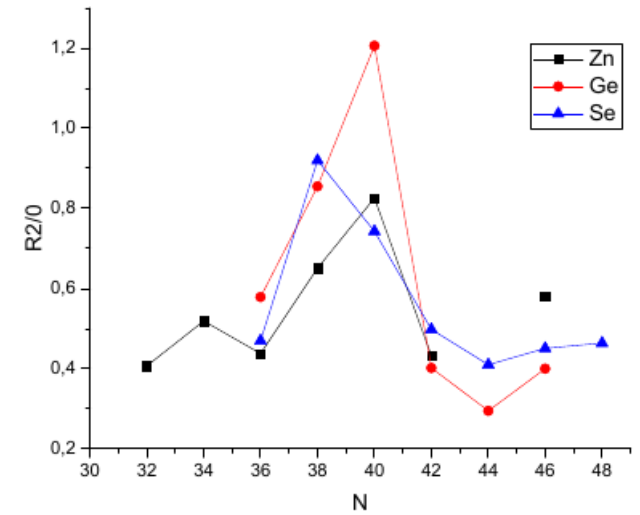
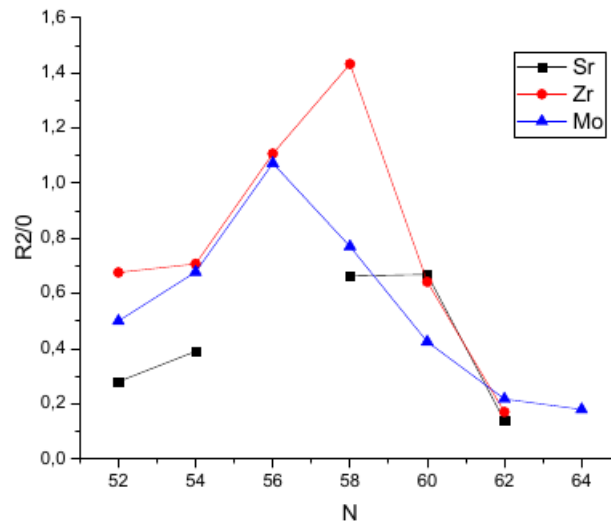
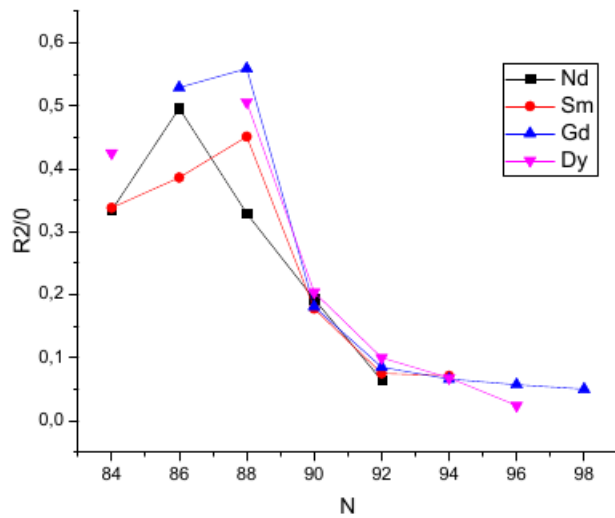
$$B(E2; 2_1^+ \rightarrow 0_1^+)$$

$$\frac{dB(E2; 2_1^+ \rightarrow 0_1^+)}{dN}(N) = B(E2; 2_1^+ \rightarrow 0_1^+)(N) - B(E2; 2_1^+ \rightarrow 0_1^+)(N-2)$$



Energy ratios $R_{2/0}$

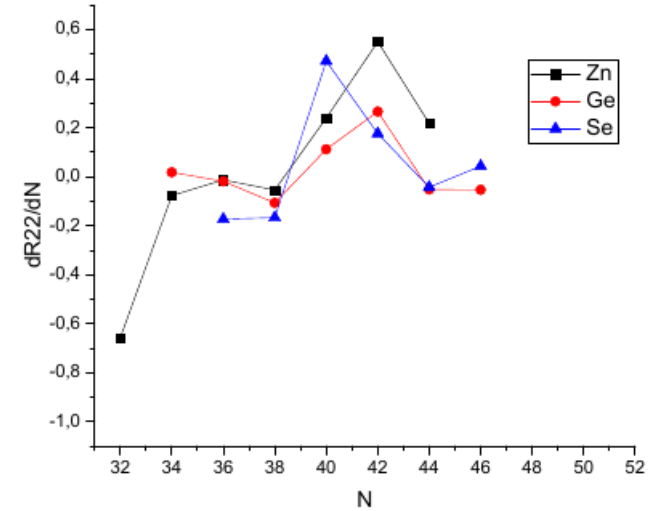
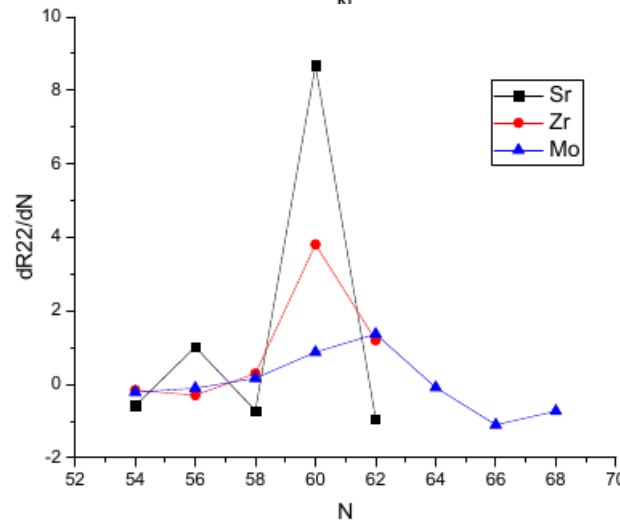
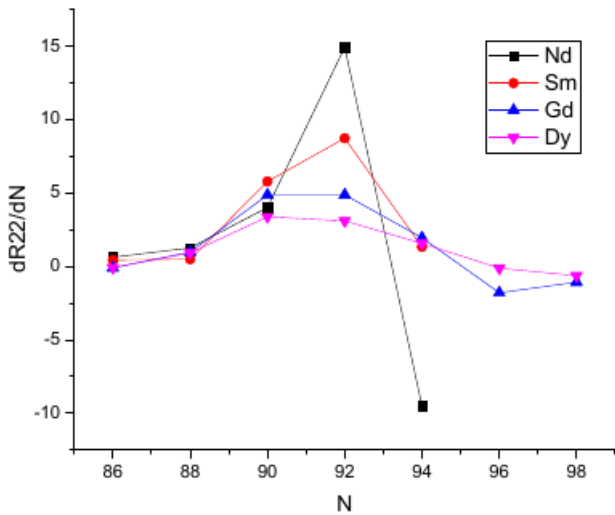
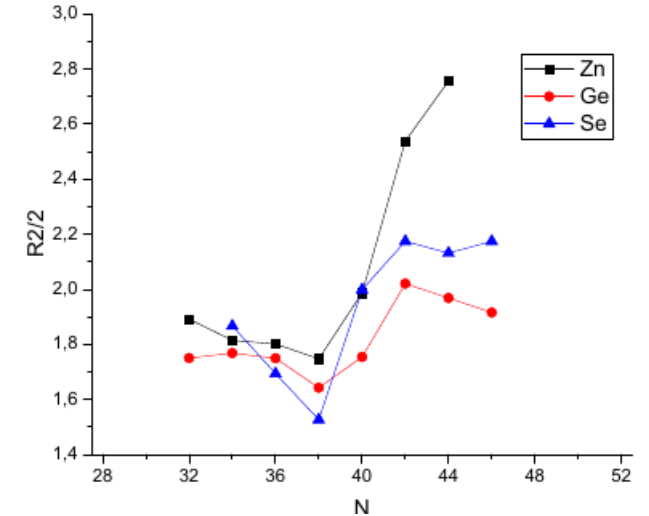
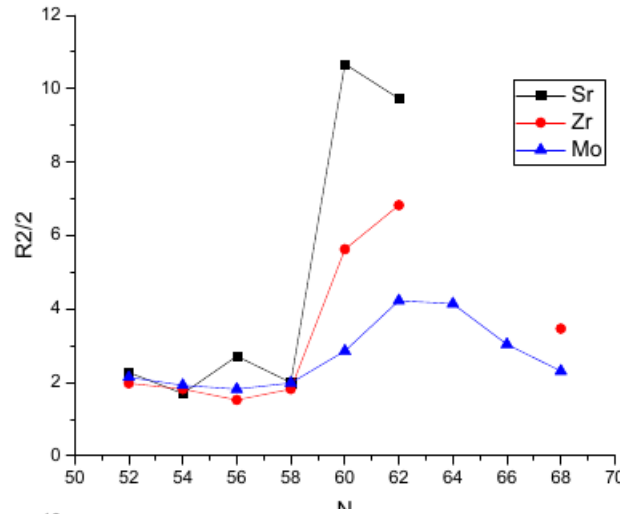
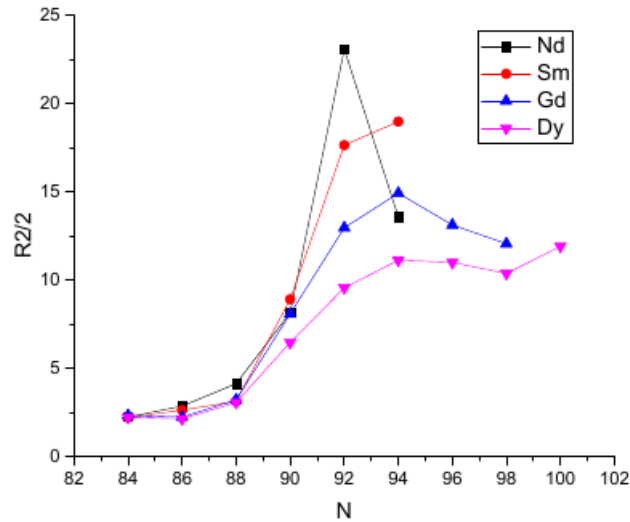
$$R_{2/0} = \frac{E(2_1^+)}{E(0_2^+)}$$



Energy ratios $R_{2/2}$

$$R_{2/2} = \frac{E(2_{\gamma}^+)}{E(2_1^+)}$$

$$\frac{dR_{2/2}}{dN}(N) = R_{2/2}(N) - R_{2/2}(N - 2)$$



A mechanism for the onset of deformation

interactions between valence protons and neutrons

midshell => increased collectivity => low-lying 2^+_1

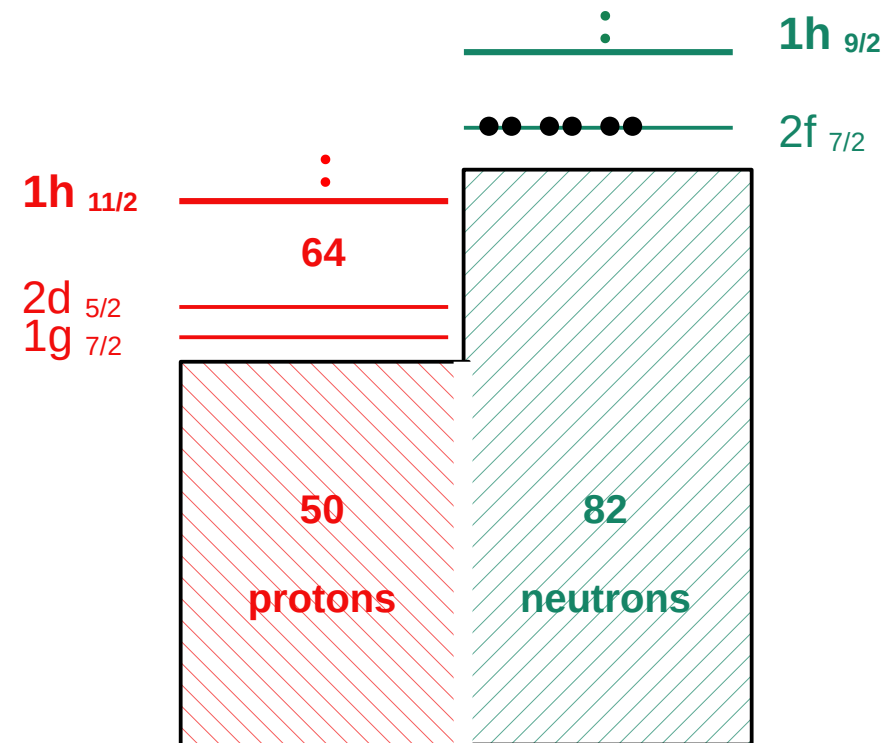
subshell structure (gaps) depend on the number of protons and neutrons present
=> *effective* shells

e.g. for $Z \approx 60$, $N \approx 90$

when $N < 90$ *effective* proton shell: $Z = 50 - 64$

=> midshell at $Z \approx 56$

=> as the neutron $h_{9/2}$ begins to fill



monopole p-n interaction between spin-orbit partner orbitals $h_{11/2}$ proton and $h_{9/2}$ neutron lowers the $h_{11/2}$ proton level, **eliminating** the $Z = 64$ gap

P. Federman and S. Pittel, Phys. Lett. B 69, 385 (1977)

R. F. Casten, Nuclear Structure from a Simple Perspective (Oxford University Press, Oxford, 1990)

T. Otsuka, Physics 4, 258 (2022)

A mechanism for the onset of deformation

when $N \geq 90$ *effective* proton shell: $Z = 50 - 82$

=> new midshell at $Z \approx 64, 66$

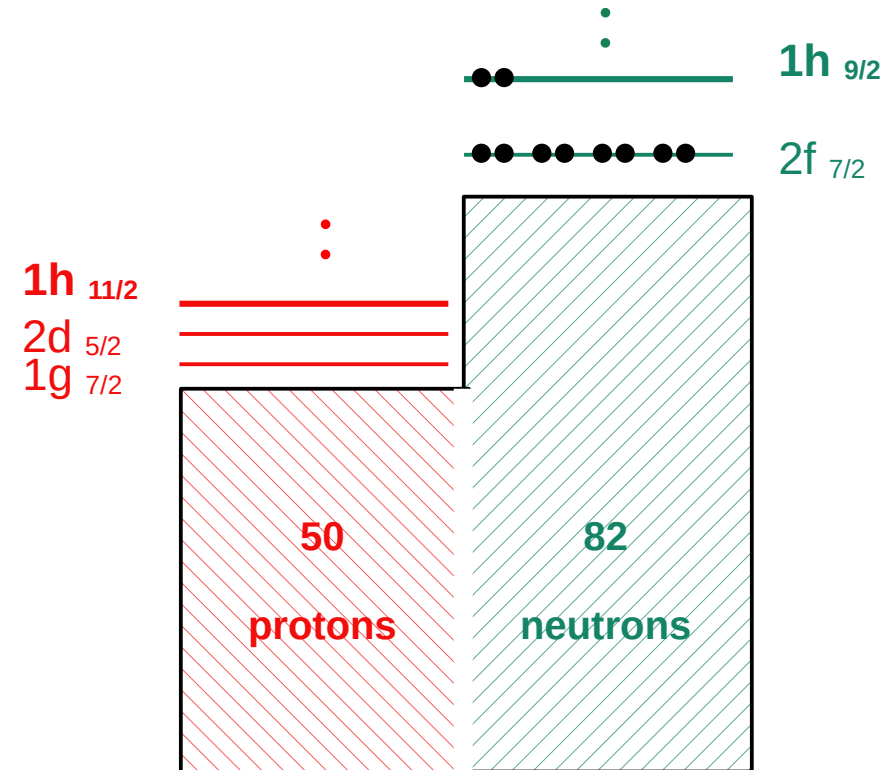
=> new position for the lowest-lying 2^+_1

=> affects nuclei with $Z = 60-66$ (Nd, Sm, Gd, Dy)

N = 88											
		258		301		334		344		358	
2^+_1 205		199									
0^+	0	0^+	0	0^+	0	0^+	0	0^+	0	0^+	0
$^{142}_{54}\text{Xe}_{88}$	$^{144}_{56}\text{Ba}_{88}$	$^{146}_{58}\text{Ce}_{88}$	$^{148}_{60}\text{Nd}_{88}$	$^{150}_{62}\text{Sm}_{88}$	$^{152}_{64}\text{Gd}_{88}$	$^{154}_{66}\text{Dy}_{88}$	$^{156}_{68}\text{Er}_{88}$	$^{158}_{70}\text{Yb}_{88}$			

N = 90																	
		181		158		130		122		123		138		192		243	
2^+_1 181																	
0^+	0	0^+	0	0^+	0	0^+	0	0^+	0	0^+	0	0^+	0	0^+	0	0^+	0
$^{144}_{54}\text{Xe}_{90}$	$^{146}_{56}\text{Ba}_{90}$	$^{148}_{58}\text{Ce}_{90}$	$^{150}_{60}\text{Nd}_{90}$	$^{152}_{62}\text{Sm}_{90}$	$^{154}_{64}\text{Gd}_{90}$	$^{156}_{66}\text{Dy}_{90}$	$^{158}_{68}\text{Er}_{90}$	$^{160}_{70}\text{Yb}_{90}$									

fig. from R. F. Casten *op.cit.*



valence nucleons also important in proxy-SU(3) scheme → talks by N. Minkov and D. Bonatsos

Microscopic calculations: SHF + BCS

$$\begin{array}{ccc} \text{Hartree-Fock} & & \text{mean-field} \\ \text{equation} & & \\ + & \longrightarrow & \hat{h}\psi_\alpha = \varepsilon_\alpha\psi_\alpha \\ \text{Skyrme} & & + \\ \text{effective interaction} & & \text{BCS} \\ & & (\varepsilon_\alpha - \epsilon_{F,q_\alpha})(u_\alpha^2 - v_\alpha^2) = \Delta w_\alpha u_\alpha v_\alpha \end{array}$$

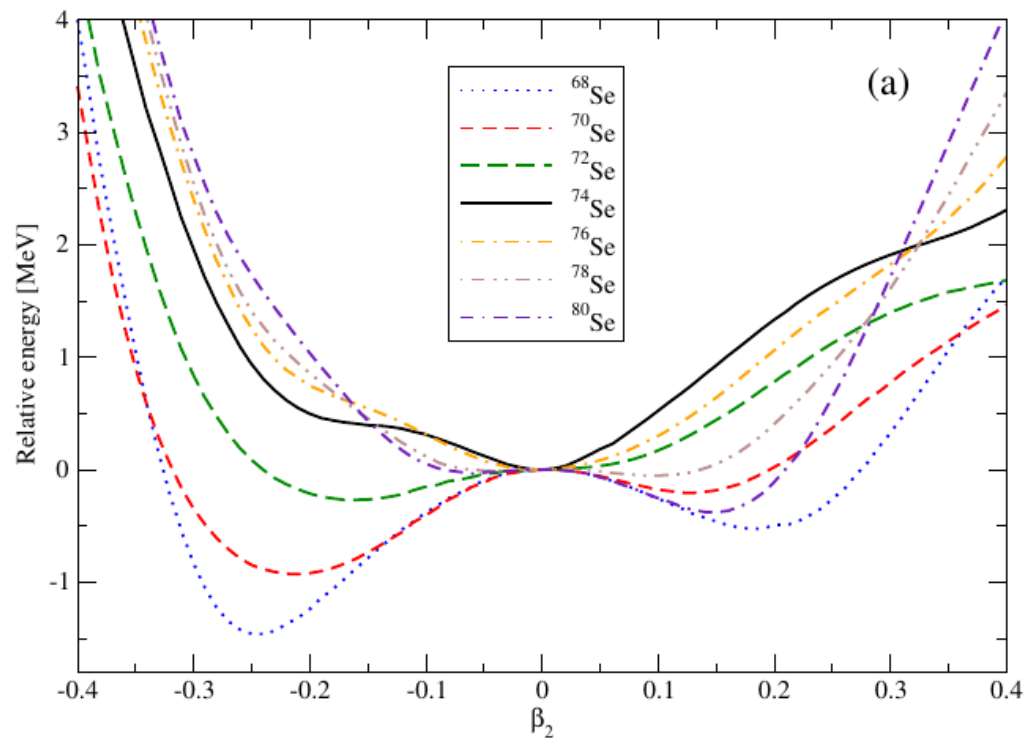
SkyAx code:
initial single particle states = Nilsson orbitals

P.-G. Reinhard, B. Schuetrumpf, and J. A. Maruhn, Comp. Phys. Comm. 258, 107603 (2021).

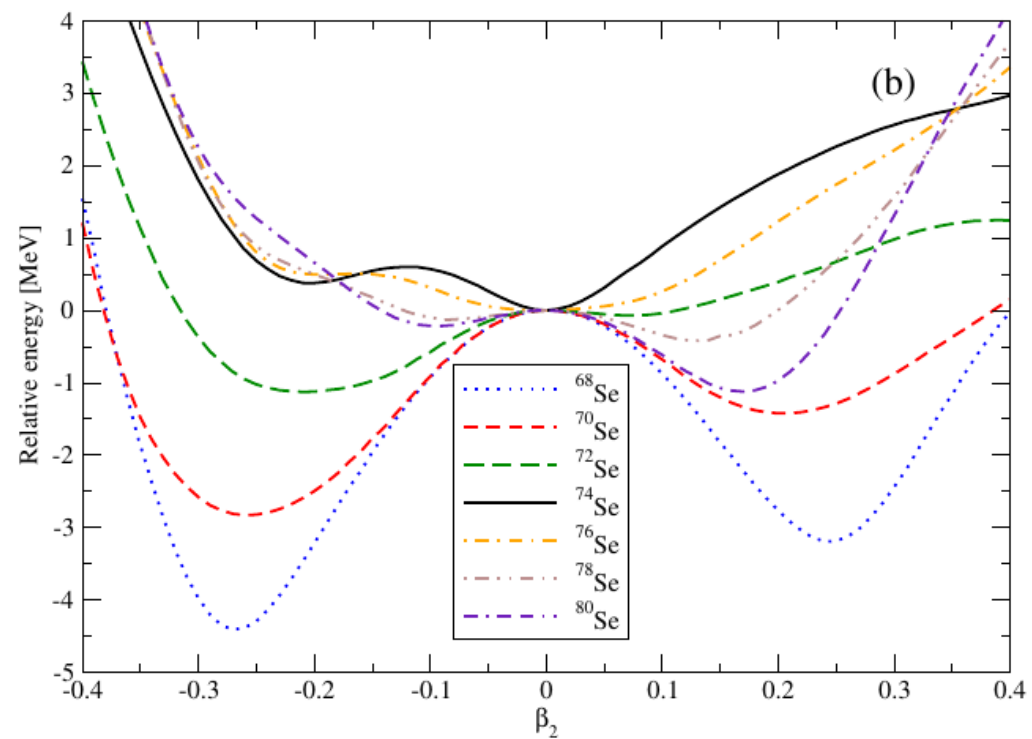
15 Skyrme parametrizations: {SV-bas, SV-tls, SV-mas07,... }

constrained calculations: (quadrupole) moment is fixed => Potential Energy Curves (PEC)

PEC for Se isotopes (N=34-46)



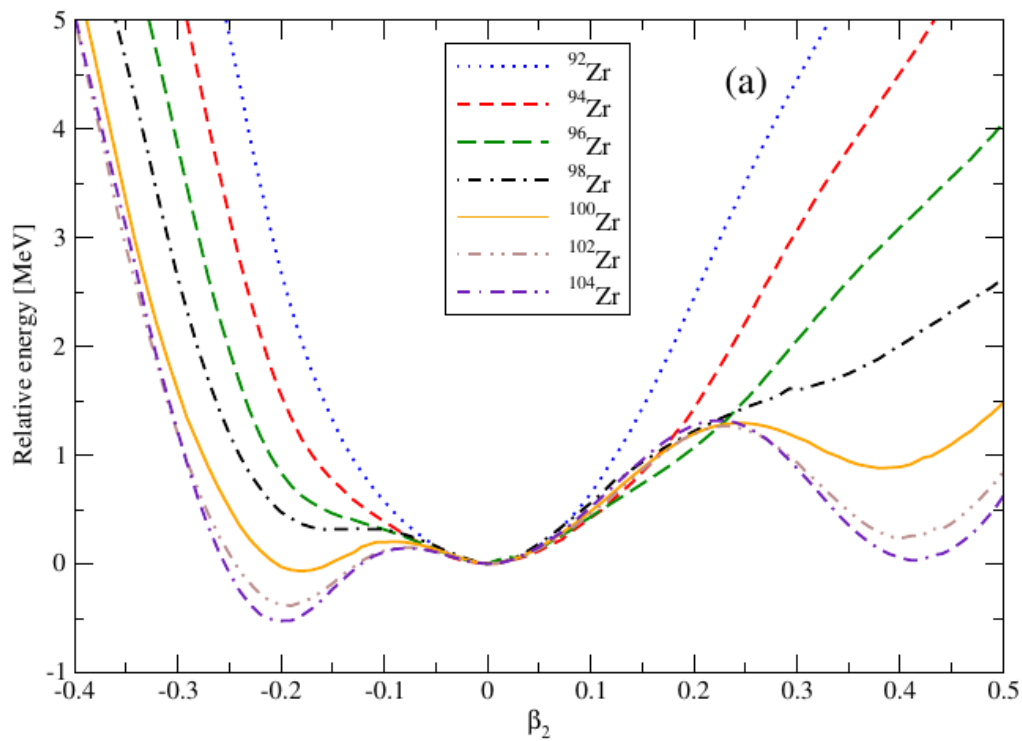
SV-bas



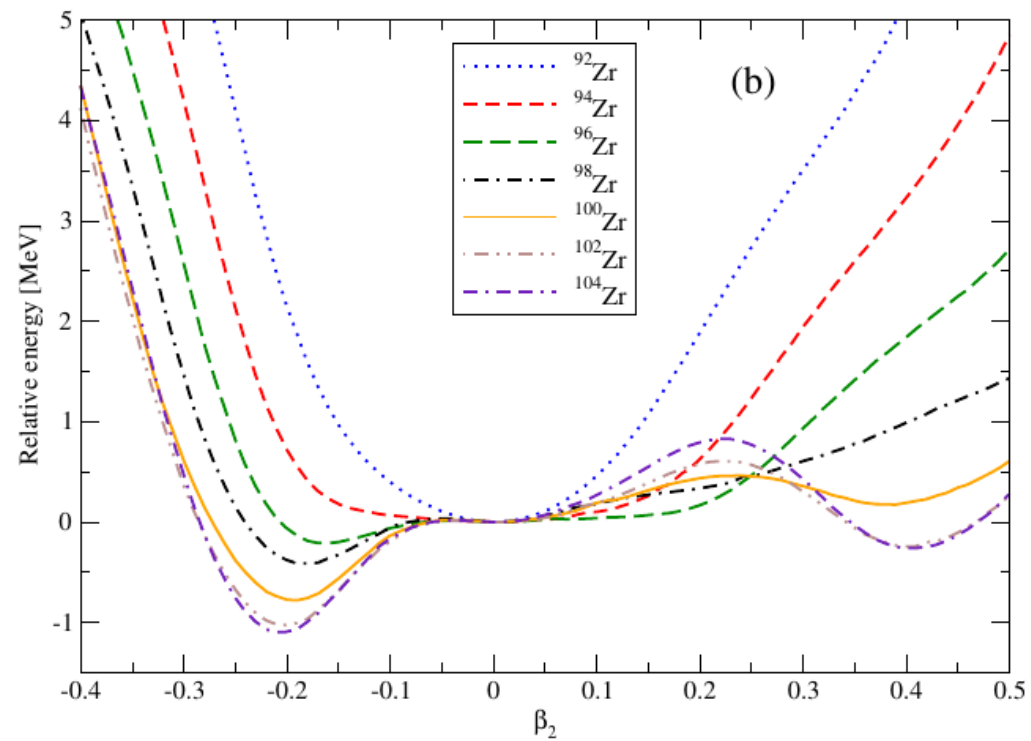
N = 40 \rightarrow ^{74}Se

SV-mas07

PEC for Zr isotopes (N=52-64)



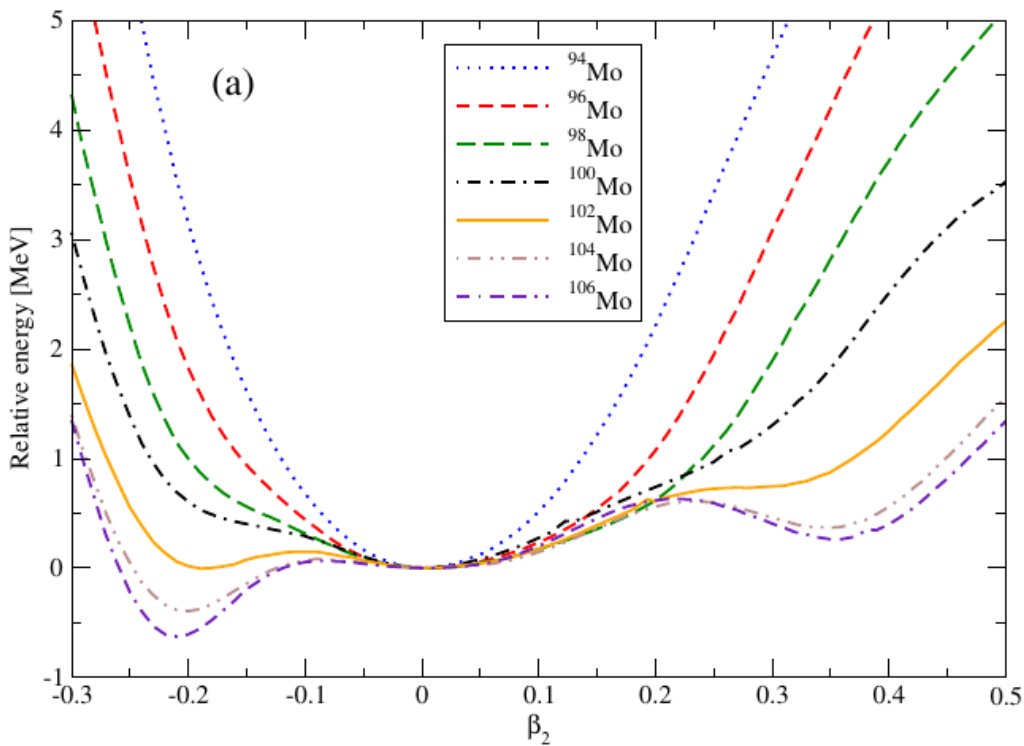
SV-bas



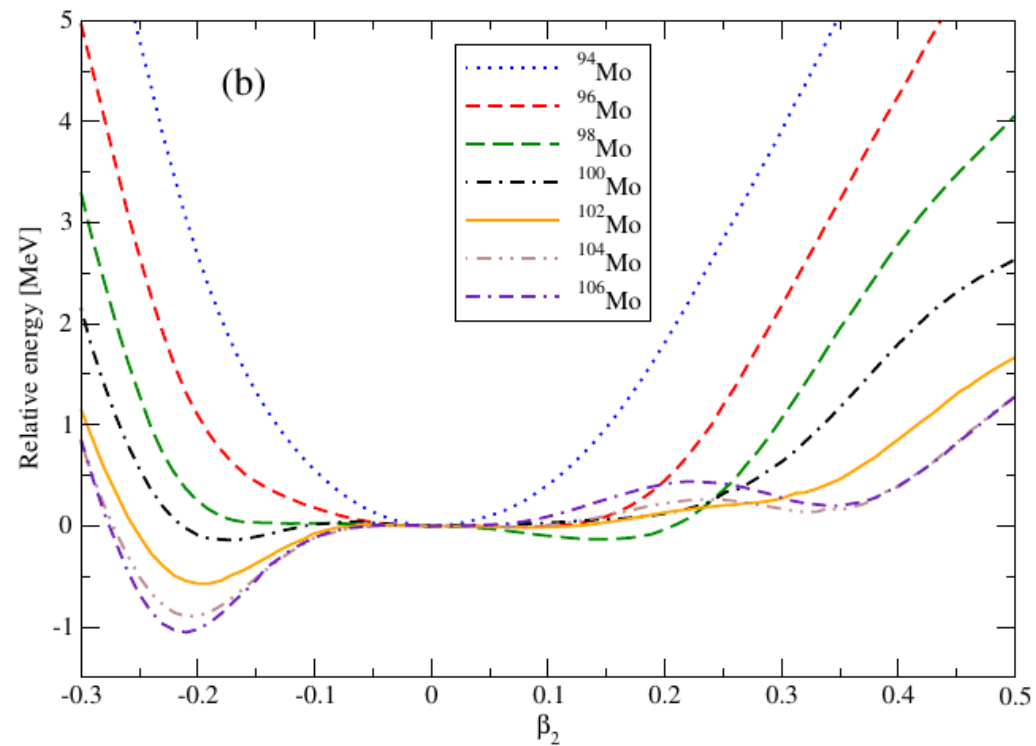
N = 60 \rightarrow ^{100}Zr

SV-mas07

PECs for Mo isotopes (N=52-64)



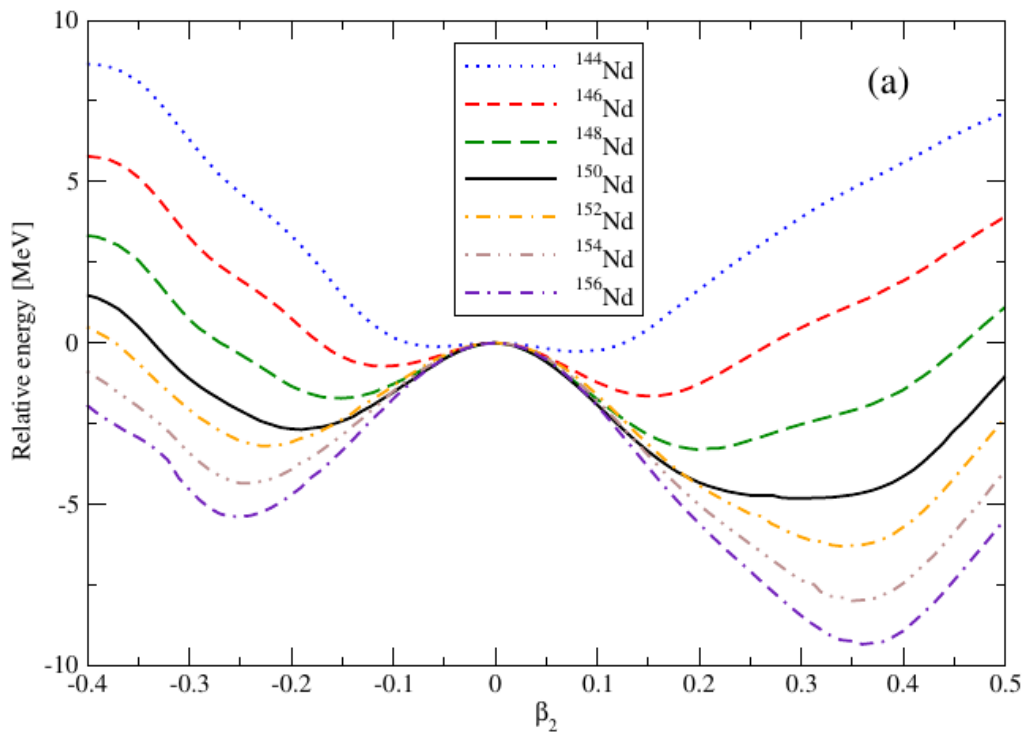
SV-bas



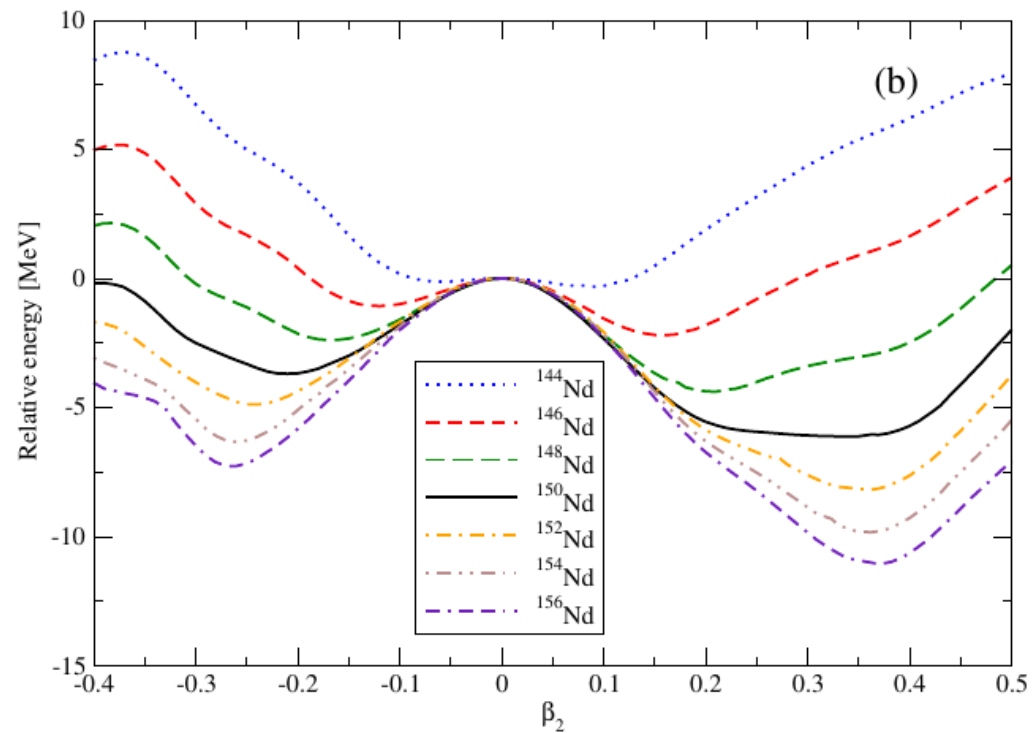
N = 60 \rightarrow ^{102}Mo

SV-mas07

PECs for Nd isotopes (N=84-96)



SV-bas



N = 90 \rightarrow ^{150}Nd

SV-mas07

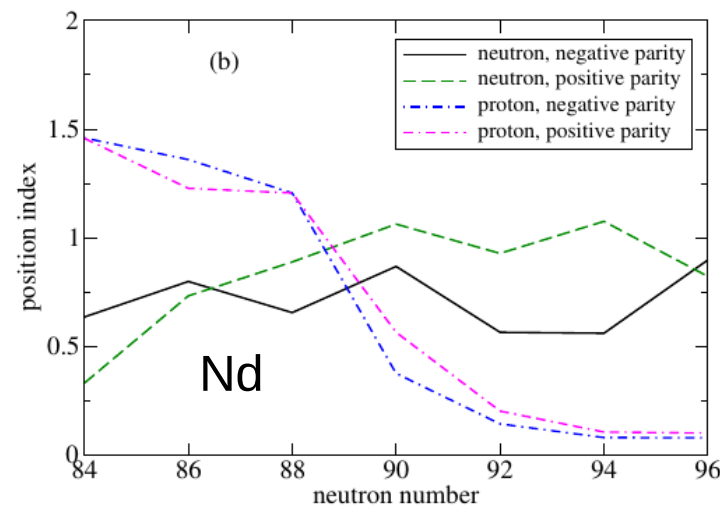
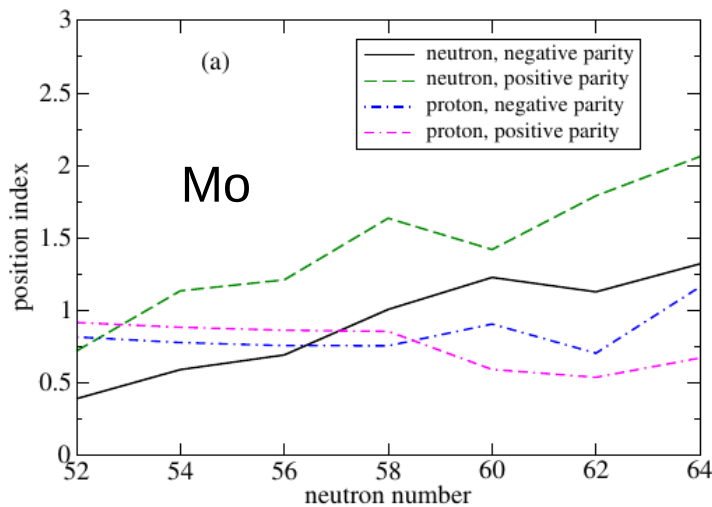
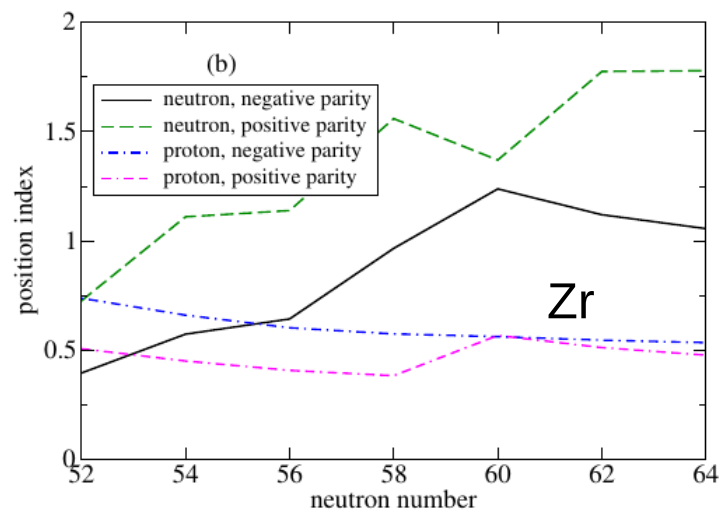
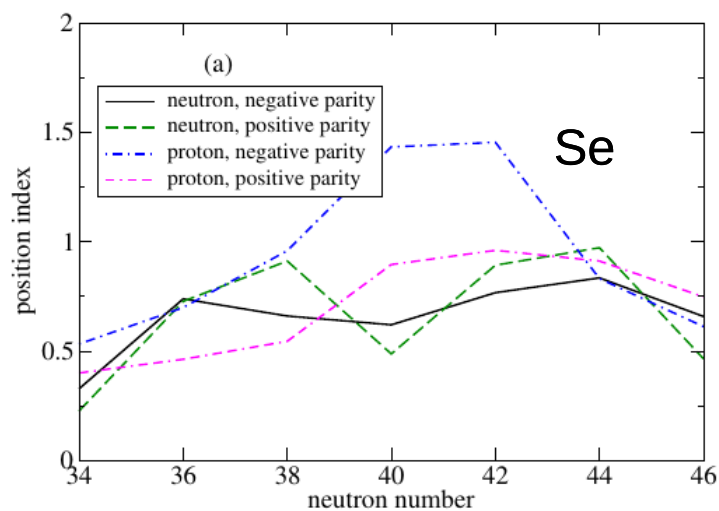
Position Index

$$I(q,\pi) = \sum_{i_{(q,\pi)}} (0.5 - |v_i^2 - 0.5|)$$

$q = n, p$ and $\pi = \pm$

v_i^2 : occupation probability of state i

what kind of levels are closest to the Fermi surface



Algebraic Collective Model (ACM)

A computationally tractable version of the collective model of **Bohr** and **Mottelson**

$$\begin{aligned} \hat{H} = & x_1 \nabla^2 + x_2 + x_3 \beta^2 + x_4 \beta^4 + \frac{x_5}{\beta^2} \\ & + x_6 \beta \cos 3\gamma + x_7 \beta^3 \cos 3\gamma + x_8 \beta^5 \cos 3\gamma + \frac{x_9}{\beta} \cos 3\gamma \\ & + x_{10} \cos^2 3\gamma + x_{11} \beta^2 \cos^2 3\gamma + x_{12} \beta^4 \cos^2 3\gamma + \frac{x_{13}}{\beta^2} \cos^2 3\gamma \\ & + \frac{x_{14}}{\hbar^2} [\hat{\pi} \otimes \hat{q} \otimes \hat{\pi}]_0 \end{aligned}$$

$$\nabla^2 = \frac{1}{\beta^4} \frac{\partial}{\partial \beta} \beta^4 \frac{\partial}{\partial \beta} + \frac{1}{\beta^2} \hat{\Lambda}$$

x_1 - x_{14} parameters: fitted to data

basis w.f.: $SU(1,1) \times SO(5) \supset U(1) \times SO(3) \supset SO(2)$

\uparrow radial β -w.f. \uparrow angular 5-dim sph. har.

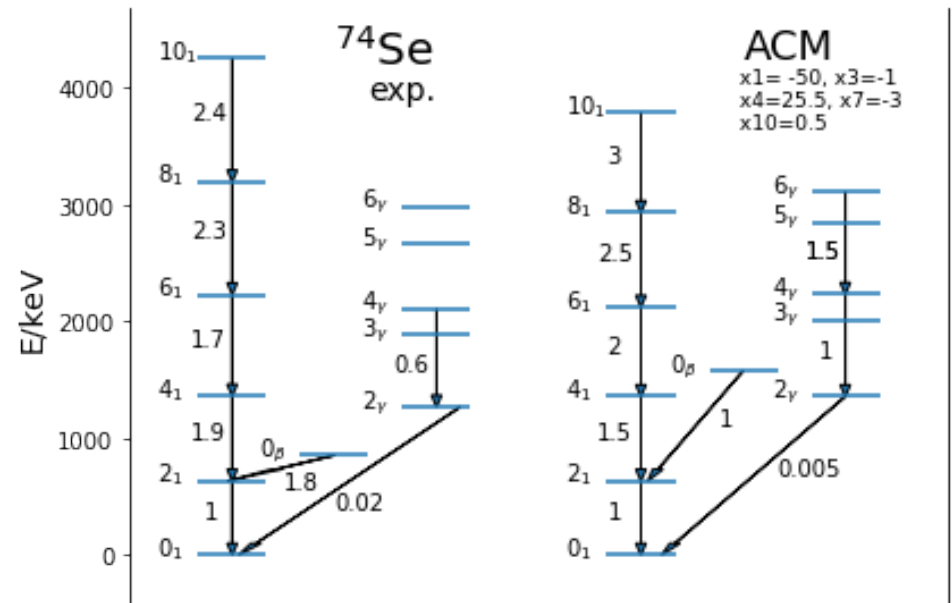
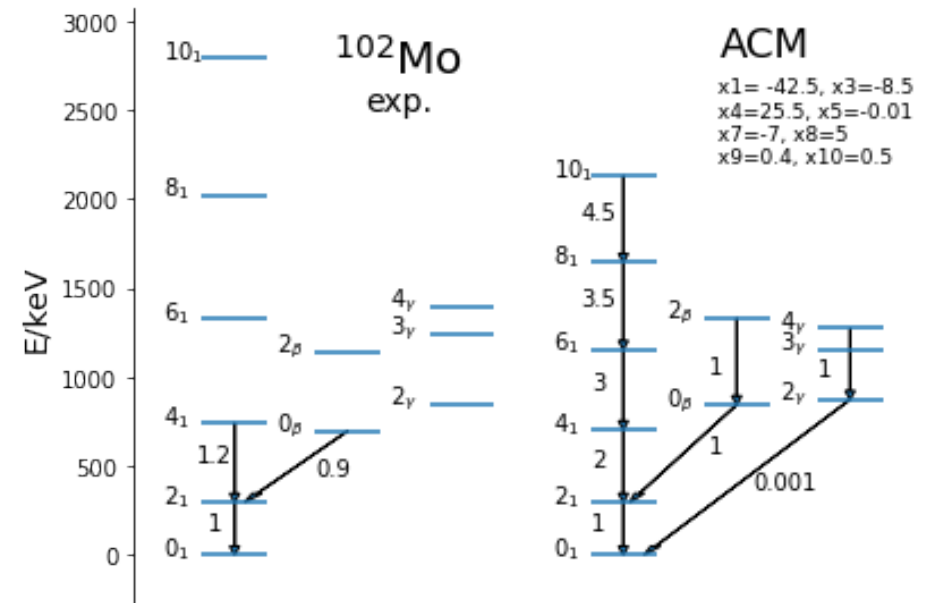
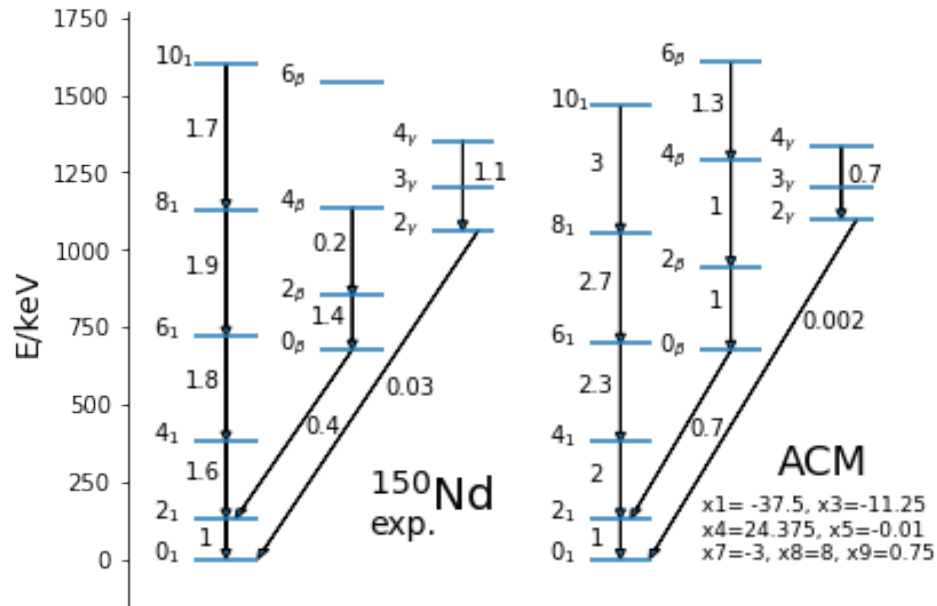
=> matrix elements
computed analytically

D. J. Rowe, T. A. Welsh, and M. A. Caprio, Phys. Rev. C 79, 054304 (2009).

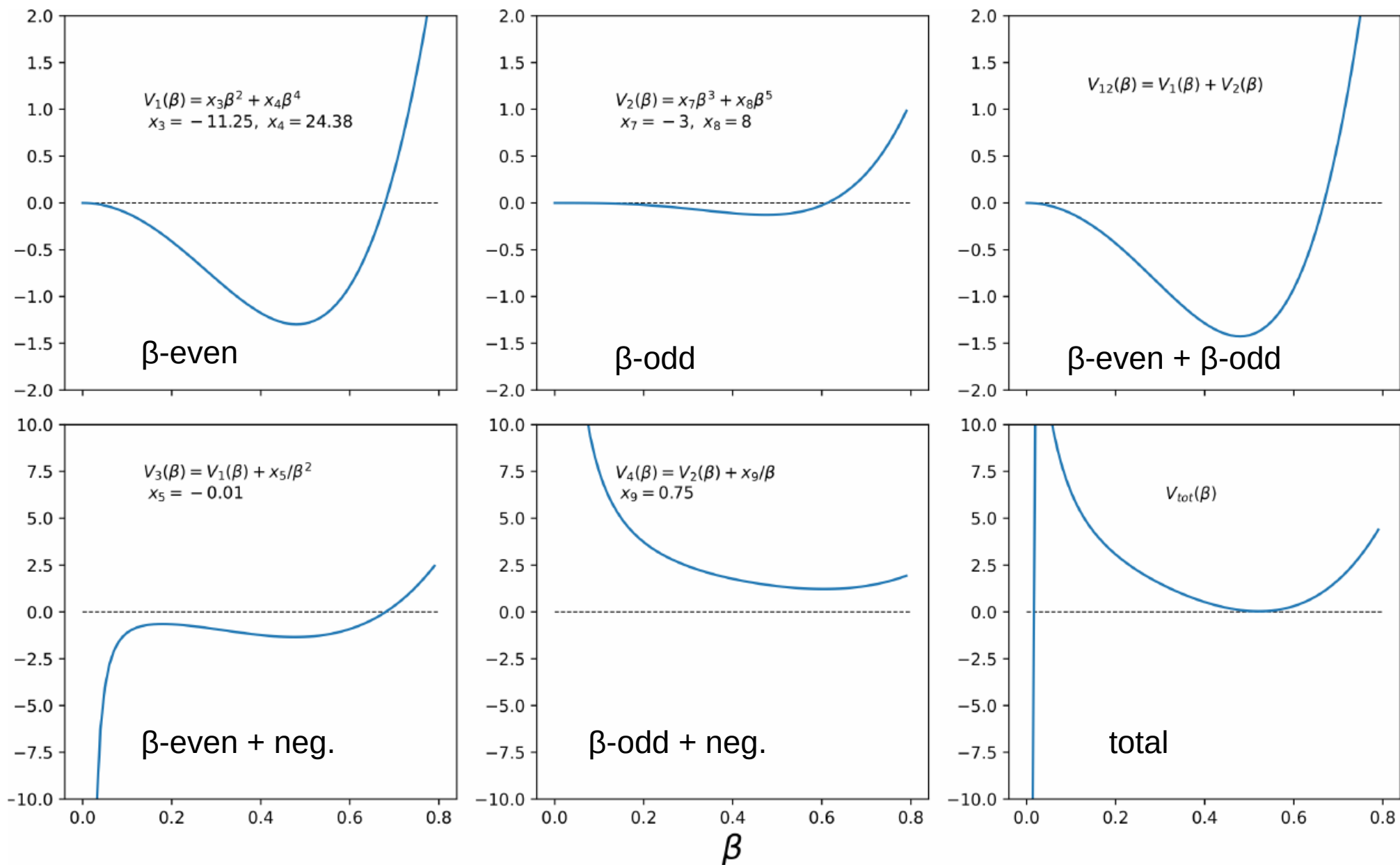
D. J. Rowe and J. L. Wood, Fundamentals of nuclear models (World Scientific, Singapore, 2010)

T. A. Welsh and D. J. Rowe, Comput. Phys. Commun. 200, 220 (2016)

ACM calculations: spectra and B(E2)s

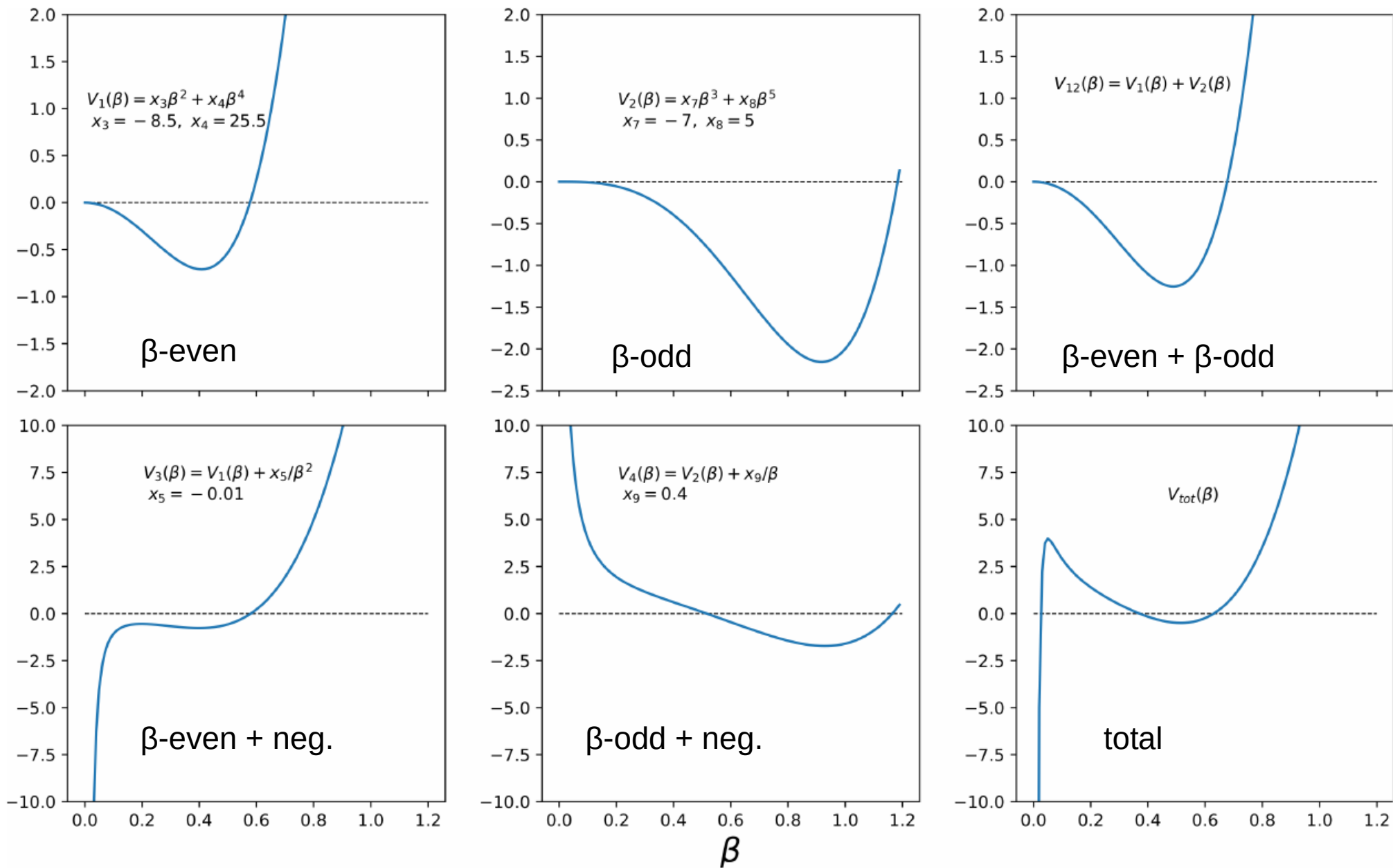


ACM Potential Energy Curves



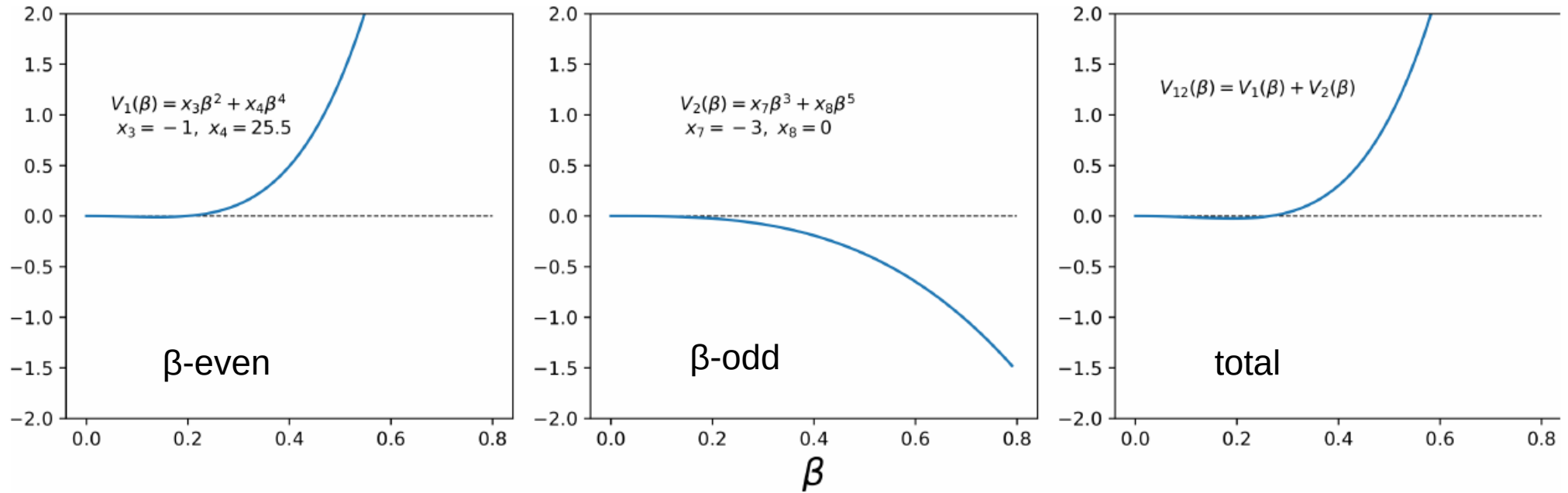
^{150}Nd

ACM Potential Energy Curves



^{102}Mo

ACM Potential Energy Curves



^{74}Se

In general, potentials resulting from ACM calculations show similarities with ones used in the Bohr Hamiltonian in the context of critical point symmetries, e.g.

- displaced infinite square well,
- infinite square well with a sloped wall,
- Davidson
- Kratzer

Summary

- Certain experimental quantities, such as energy ratios: $R_{4/2}, \dots$ and $B(E2)$ transition rates serve as **benchmarks** for nuclear structure
- Valence **p-n** interactions driving force for structural change
- Microscopic calculations in the **$N = 40, 60, 90$** regions show signs of a *first-order* phase transition with coexisting minima in the PECs
- Potentials resulting from the ACM calculations show similarities with ones used in the context of the Bohr Hamiltonian (critical point symmetries)

TOPICAL REVIEW

Quantum phase transitions and structural evolution in nuclei

R F Casten and E A McCutchan

Wright Nuclear Structure Laboratory, Yale University, New Haven, CT 06520, USA

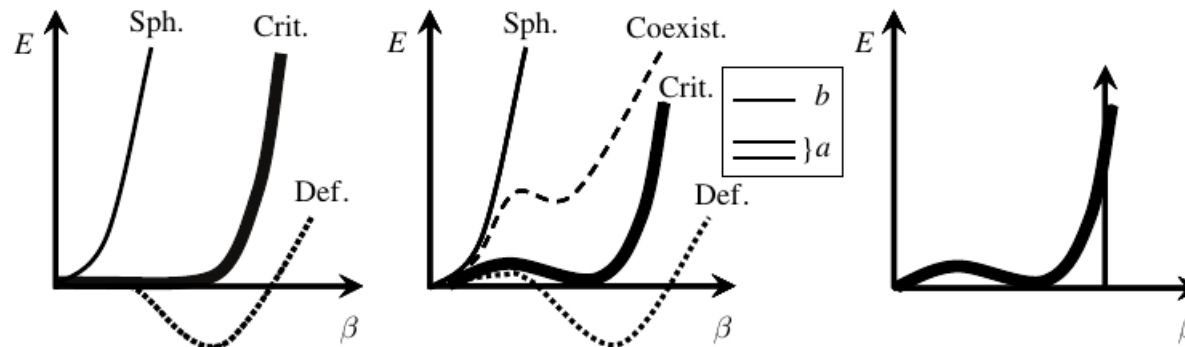


Figure 7. Energy surfaces for nuclei with successively larger numbers of valence nucleons plotted against the quadrupole deformation β (left) for a second-order phase transition and (middle) for a first-order phase transition. Right: the curve ‘Crit.’ repeated along with the square well ansatz that embodies the essential features of X(5) and E(5). The inset to the middle figure represents a set of shell model orbits a and b .

